J. Fluid Mech. (1970), *vol.* 40, *part* 2, *pp.* 361–384
Printed in Great Britain

Some dynamical effects of heat on a turbulent boundary layer

By C. I. H. NICHOLL
Cavendish Laboratory, University of Cambridge†

(Received 2 June 1969)

The dynamical effects of a sudden increase of as much as 100 °C in boundary temperature upon fully turbulent boundary layers at low Reynolds numbers in air have been investigated in a wind tunnel. A section of the floor or the roof of the tunnel could be heated, so that the rate of working of gravitational forces on the turbulence could be made to represent either a gain or a loss of turbulent mechanical energy. Techniques of hot-wire anemometry were employed which enabled the instantaneous temperature and the instantaneous velocity to be measured simultaneously at a point in the non-homogeneous turbulent flow field.

In the case of a strong discontinuity in the floor temperature, a fine-scale convective structure developed from the highly unstable interface between the heated air just above the surface and the turbulent boundary layer; and the motion in this region was sufficiently vigorous that the mean pressure in the vicinity of the floor was reduced and a local wall jet was generated. The deduced pressure distribution is regarded as evidence of coupling between the free and forced convection modes which may lead to a series of local wall jets downstream of the discontinuity.

In the case of a strong discontinuity in the roof temperature, the interface between the heated air and the turbulent boundary layer was stable; and the boundary-layer turbulence, acting to spread this stable gradient over the vertical extent of the boundary layer, was required to do work against the gravitational field. A rate of working against gravity which was an order of magnitude less than the rate of supply of turbulent energy from the mean shear proved sufficient to suppress the turbulence in a very short time.

1. Introduction

The dynamical effects of the density gradients produced by heating or cooling the solid bounding surface of a turbulent shear flow are usually neglected in calculations of the turbulent transport across the flow. However, there are many situations in which this assumption that the flux of heat through the turbulent boundary layer is without effect upon the structure of the turbulence is no longer valid.

For example, the radiative cooling of the earth's surface at sunset on a clear night is often accompanied by a sudden decrease in the gustiness of the surface

† Present address: Department of Mechanical Engineering, Laval University, Quebec.

wind, that is, by a decrease in the intensity of turbulence in the atmospheric boundary layer. Richardson (1920) pointed out that this phenomenon must be due to the extra work required of the turbulence by the density gradient imposed on the boundary layer by the cold surface. Though very little was known at that time about the structure of turbulent shear flows, he discussed the possible sources and sinks for turbulent energy with remarkable insight. In order to circumvent the lack of experimental information about the diffusion and dissipation mechanisms in fully turbulent shear flow, he considered finally a large vertical section of the atmosphere in which the winds were of a constant mean velocity in a given horizontal plane, and very slightly and uniformly turbulent. Under these conditions, the turbulent intensity level would be stable if the rate of work against gravity required of the eddies were equal to the rate of production of turbulent energy by the mean shear. A non-dimensional number formed from the ratio of these rates is called a Richardson number.

Richardson numbers encountered in the literature are of two types. The first type is intended to characterize an entire flow field. For example, if it were possible to take account of the turbulent transport processes for heat and momentum by a single virtual transfer coefficient K, associated with diffusion down suitably-chosen average gradients which were characterized by scales U_0, $\Delta\phi_0$ and l_0 of velocity, potential temperature and length respectively, then the global Richardson number for the section of the atmosphere considered by Richardson would be $R = g.\Delta\phi_0.l_0/U_0^2.T_0$, where T_0 is a mean absolute temperature. The conditions which must be satisfied if R is to be the only global parameter governing dynamical similarity in the flow are derived in detail by Batchelor (1953).

Alternatively, a local Richardson number may be defined. The so-called 'flux' Richardson number, R_f, is formed from the ratio of the conventional expressions for the local rate of working of the turbulence against gravity $g_i\overline{\rho' u_i}$ and the local rate of production of turbulent energy $\rho\overline{u_i u_j}.\partial U_i/\partial x_j$, where ρ' is the fluctuation of the density from the mean ρ, U_i and u_i are the i components of the mean fluid velocity and the fluctuation about it, and repeated suffices indicate summation over the three possible values of the repeated suffix. If local virtual transfer coefficients for mass (K_s) and momentum (K_m) can be employed, then a local 'gradient' Richardson number can be defined which, for a two-dimensional shear flow, would be written $K_s(g/\rho)(\partial\rho/\partial z)/K_m(\partial U/\partial z)^2$. In general, the value of a local Richardson number will not be the same at all points in a turbulent shear flow, and measurements of 'critical' values of local Richardson numbers obtained in marginally stable† inhomogeneous flows serve as a guide to the turbulent structure rather than as an indication of the stability of the turbulent intensity level. Nevertheless, several attempts have been made to express local Richardson numbers in terms of the global parameters of the flow (such as R) and some general features of turbulent motion.

For example, Ellison (1957) considered a boundary layer of the atmospheric

† Marginally stable in this context means that the turbulence is transporting the maximum possible weight flux against the gravitational field, for a given U_0 and T_0.

type, through which the shear stress and heat flux were assumed constant. Unlike Richardson's flow, Ellison's theoretical model included the dissipative mechanisms found in fully developed turbulent shear flow; and in order to place an upper limit on the value of R_f in the turbulent flow, he was forced to introduce hypotheses concerning the rates at which these dissipative mechanisms would begin to destroy the turbulent energy, the density fluctuations and the correlation coefficient $\overline{w\rho'}/\sqrt{\overline{w}^2}\sqrt{\overline{\rho}'^2}$ (where w is the component of the fluctuating velocity in the direction of the gravitational field) as the vertical inhomogeneity exceeded the critical value. He postulated that the ratios between these rates remain constant during the decay of the turbulence, or in other words, that the process of the decay of each quantity is dominated by roughly the same length and velocity scales. Under these conditions, he was able to predict that vertical flux of mass would cease if R_f reached a value of 0·15. He concluded that, in highly stablizing gradients, buoyancy forces act to change the scale and structure of the motion, rather than directly on the turbulent energy.

At about the same time, Townsend (1957) examined the situation in a stably stratified, developing free turbulent shear flow, where the inhomogeneity of the turbulence lay in the direction of flow rather than in the direction of shear. In cases where advection of turbulent energy could be neglected, and the Reynolds stress was uniform, dimensional reasoning suggested that the ratio of turbulent energy loss to turbulent energy production, considered as a function of turbulent energy level, must have a minimum; and if for given mean gradients this minimum were greater than unity, the turbulence must decay. Under the same sort of restrictions as Ellison imposed upon the effect of stabilizing gradients on the turbulent structure, Townsend was able to use this idea to set limits upon the value of R_f if a turbulent intensity were to be found to satisfy the energy equation. His analysis gave $R_f < \frac{1}{2}$.

In these and other analyses of stably stratified turbulent shear flows which have been published, it is assumed that the entire dynamical effect of heat fluctuations on the turbulence is comprised in the weight flux term $\overline{w\rho'}.g$, which represents the work done during turbulent diffusion of weight fluctuations against the gravitational field. The fluid is supposed to be of uniform density but variable weight.

Up to the present, there has been very little detailed experimental information available to guide the theoretician as to the structural changes which may be introduced in turbulent shear flow by strong heating. The purpose of this paper is to provide some data to help to fill this gap. It must be emphasized from the outset that the flow configuration in which the measurements were obtained was essentially inhomogeneous, in the direction of flow as well as in the direction of shear, and that similarity analyses are therefore unlikely to bear fruit, except in restricted domains of the flow.

2. The equations governing the motion

The configuration studied experimentally was that of a two-dimensional turbulent boundary layer flow of air in the x direction over a horizontal surface

normal to z. This boundary layer encountered a discontinuity in surface temperature. Only velocities and temperatures were measured. In deriving the equations used in the analysis of the experimental observations, therefore, the assumption

$$\rho = p/RT \approx p_0/RT, \tag{2.1}$$

$$\rho' = -\theta.\rho/T = -\theta.p_0/RT^2 \tag{2.2}$$

was introduced, where θ is a temperature fluctuation about the mean absolute temperature T, p is the mean local pressure and p_0 is the reference pressure outside the boundary layer. At the very low Mach number of the flow, the pressure variations were assumed negligible compared with the absolute pressure. However, the *gradient* of pressure was not necessarily negligible in the equations of conservation of momentum, and the correlations between fluctuating pressure and velocity were dominant in some regions of the flow. The temperature rise due to viscous dissipation was negligible compared with the temperature differences imposed on the flow. Under these conditions, the equations governing the flow are:

$$\frac{\partial(U/T)}{\partial x}+\frac{\partial(W/T)}{\partial z}-\frac{\partial(\overline{\theta u}/T^2)}{\partial x}-\frac{\partial(\overline{\theta w}/T^2)}{\partial z}=0, \tag{2.3}$$

$$\frac{p_0}{R}\left[\frac{\partial}{\partial x}\left(\frac{U^2+\overline{u^2}}{T}-2\frac{U\overline{u\theta}+\overline{u^2\theta}}{T^2}\right)+\frac{\partial}{\partial z}\left(\frac{UW+\overline{uw}}{T}-\frac{U\overline{\theta w}+W\overline{\theta u}+\overline{\theta uw}}{T^2}\right)\right]$$
$$+\frac{\partial p}{\partial x}-\mu\left(\frac{\partial^2 U}{\partial x^2}+\frac{\partial^2 U}{\partial z^2}\right)=0, \tag{2.4}$$

$$\frac{p_0}{R}\left[\frac{\partial}{\partial x}\left(\frac{WU+\overline{wu}}{T}-\frac{W\overline{\theta u}+U\overline{\theta w}+\overline{uw\theta}}{T^2}\right)+\frac{\partial}{\partial z}\left(\frac{W^2+\overline{w^2}}{T}-2\frac{W\overline{\theta w}+\overline{w^2\theta}}{T^2}\right)\right]$$
$$+\frac{\partial p}{\partial z}+\frac{p_0.g}{RT}-\mu\left(\frac{\partial^2 W}{\partial x^2}+\frac{\partial^2 W}{\partial z^2}\right)=0, \tag{2.5}$$

$$\frac{C_v.p_0}{R}\left[\frac{\partial}{\partial x}\left(U-\frac{U\overline{\theta^2}+\overline{u\theta^2}}{T^2}\right)+\frac{\partial}{\partial z}\left(W-\frac{W\overline{\theta^2}+\overline{w\theta^2}}{T^2}\right)\right]+\frac{\partial}{\partial x}\left(-K\frac{\partial T}{\partial x}\right)$$
$$+\frac{\partial}{\partial z}\left(-K\frac{\partial T}{\partial z}\right)+p\left[\frac{\partial U}{\partial x}+\frac{\partial W}{\partial z}\right]+\overline{p'\frac{\partial u_i}{\partial x_i}}=0, \tag{2.6}$$

$$\frac{p_0}{R}\left[\frac{\partial}{\partial x}\left(\frac{U\overline{q^2}+\overline{uq^2}}{2T}-\frac{U}{2T^2}\overline{\theta q^2}\right)+\frac{\partial}{\partial z}\left(\frac{W\overline{q^2}+\overline{wq^2}}{2T}-\frac{W}{2T^2}\overline{\theta q^2}\right)+\left(\frac{\overline{u^2}}{T}-\frac{U\overline{\theta u}+\overline{\theta u^2}}{T^2}\right)\frac{\partial U}{\partial x}\right.$$
$$+\left(\frac{\overline{uw}}{T}-\frac{W\overline{\theta u}+\overline{\theta wu}}{T^2}\right)\frac{\partial U}{\partial z}+\left(\frac{\overline{uw}}{T}-\frac{U\overline{\theta w}+\overline{\theta wu}}{T^2}\right)\frac{\partial W}{\partial x}$$
$$\left.+\left(\frac{\overline{w^2}}{T}-\frac{W\overline{\theta w}+\overline{\theta w^2}}{T^2}\right)\frac{\partial W}{\partial z}-\frac{\overline{\theta w}}{T^2}g\right]+\overline{u_i\frac{\partial p'}{\partial x_i}}-\mu\overline{u_i\nabla^2 u_i}=0, \tag{2.7}$$

where p' is a fluctuation from the local mean pressure and $\overline{q^2}=\overline{u^2}+\overline{v^2}+\overline{w^2}$. The effects of gradients in the coefficient of viscosity have been neglected, as has any influence of a 'second' coefficient of viscosity. C_v has been used in (2.6) in preference to C_p in order to set out more explicitly the different contributions to

the heat balance, in a flow in which the density and temperature differences are not small and work of expansion on a turbulent scale is significant.

The mass balance equation (2.3) shows that in the turbulent flow of air $\overline{w\theta}$ represents a flux of *mass*, not, as would appear from the usual constant-density analysis, a flux of heat. We have also to remember that the identification of a correlation such as $\overline{w\theta}$ with a flux assumes that a fluid tatter, once transported across the plane of measurement by turbulent motion, is mixed into its surroundings by a molecular diffusion whose effects are magnified by the intense vorticity characteristic of turbulence. In strongly stabilizing density gradients, it is possible that perturbation velocities will be associated with gravity wave-like motions, in which the vorticity would be much less intense than in turbulence. Molecular diffusion rates would be relatively weak in such motions, and the correlation would yield an exaggerated estimate of the mass flux. The same remark would apply to correlations representing the vertical transport of any quantity for which the mixing process is controlled by molecular diffusion rates.

The momentum equations (2.4) and (2.5) contain extra terms of the type $U.\overline{w\theta}$ and $\overline{u^2\theta}$ which represent the contributions of the turbulent mass flux to the momentum blance. The vertical pressure distribution does not in general correspond to hydrostatic equilibrium.

The heat balance (2.6) shows that the turbulent velocities may influence transport of heat in the boundary layer in two ways, by their effect on the divergence of the mean flow, and by establishing gradients of intensity of temperature fluctuations $\overline{\theta^2}$ in the flow. The divergence of the mean flow also introduces a work of expansion term $p(\partial U/\partial x + \partial W/dz)$; and the corresponding turbulent terms $\overline{p'\partial u_i/\partial x_i}$ represent a direct transformation of thermal energy into kinetic energy on a turbulent scale. The correlation $\overline{w\theta}$ does not appear in the heat balance. In consequence of the approximation (2.1), the mean thermal energy per unit volume, $C_v.\rho.T$ is constant throughout the heated boundary layer (neglecting any temperature dependence of C_v). In a fluctuating field, the first term of the equation (2.6) is, before approximation, $C_v(\partial/\partial x)(\rho.T.U + \rho.\overline{\theta u} + T.\overline{\rho' u} + U.\overline{\rho'\theta} + \overline{u\rho'\theta})$. Substituting for ρ and ρ' from (2.1), (2.2), the second term $(p_0/RT)\overline{\theta u}$ is cancelled out by the third $T.-\overline{\theta(p_0/RT^2)u}$. A similar substitution eliminates $\overline{w\theta}$.

In the turbulent energy balance (2.7), variations in density are seen to introduce additional terms in the expressions for advection and production of turbulent energy, and pressure-velocity correlation turns up as a source term.

3. Experimental arrangements

The experiments were carried out in a small open-circuit wind tunnel in the Cavendish Laboratory at free-stream velocities between 150 and 240 cm/s. The boundary layer was tripped at the downstream end of the contraction (figure 1), at a distance of 127 cm upstream from the beginning of the heated surface. The displacement thickness Reynolds number of the turbulent boundary layer at the upstream end of the heated surface ($x_h = 0$) was about 600.

Mean velocity and mean temperature in the boundary layer were measured with the same single transverse wire, connected in a Wheatstone bridge. For temperature measurements, the bridge was driven by an alternating current, and the bridge out-of-balance voltage was measured with a very sensitive detector, so that the bridge current could be kept well below the level where it would heat the wire appreciably.

The basis of the technique of measuring r.m.s. quantities rests upon the fact that the sensitivity of the rate of heat loss from the anemometer wire to a change in ambient air *temperature* increases more slowly with increasing wire temperature

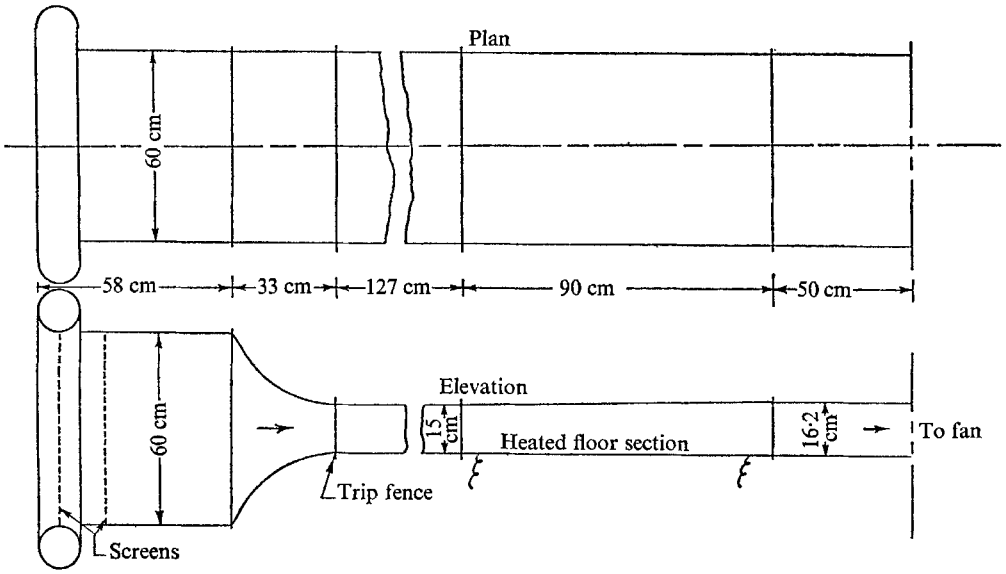

FIGURE 1. Wind tunnel.

than does the corresponding sensitivity to a change in the *velocity* of the ambient air stream. In a flow field where both temperature and velocity fluctuations were present, therefore, a warm wire, operated at perhaps 15 °C above mean ambient temperature, was sensitive primarily to ambient *temperature* fluctuations, whereas a hot wire, operated at 150 °C above ambient temperature, was sensitive primarily to fluctuations in the *velocity* of the air stream passing over the wire.

Townsend (1951) has pointed out that if, for the single hot wire of the ordinary anemometer, one substitutes two identical wires, parallel and as close together as possible, and operated at temperatures of, say 15 °C and 150 °C above mean ambient temperature, it is then possible, by subtracting appropriate fractions of the fluctuating voltage output of the hot wire from the whole of the fluctuating voltage output of the warm wire, to obtain simultaneously signals corresponding to instantaneous pure temperature fluctuation and instantaneous pure velocity fluctuation, respectively, at the wire assembly position. This scheme has the great advantage that double and triple correlations can be formed immediately from the signals.

The bridge circuit of figure 3 was designed to produce the pure temperature and pure velocity fluctuation signals from the potentiometer terminals marked temp and vel respectively.

If K_u and K_θ are the sensitivities of a correctly compensated hot-wire anemometer to ambient velocity and temperature fluctuations, respectively, we may write for each wire

$$\frac{e}{i.R} = K_u.\frac{u}{U} + K_\theta.\frac{\theta}{T}, \tag{3.1}$$

where e is the voltage fluctuation obtained from a wire of resistance R through which a heating current i is passing.

In order to obtain, for example, a signal independent of ambient air temperature fluctuation, one set the velocity potentiometer to subtract a fraction f_v of the total hot wire signal from the whole of the warm wire signal, where $f_v = (K_\theta.i.R)_w/(K_\theta.i.R)_h$. Then a temperature fluctuation θ applied to the pair of wires would produce a signal at the velocity terminal

$$e_v = [(K_\theta.i.R)_w - f_v(K_\theta.i.R)_h]\frac{\theta}{T} = 0, \tag{3.2}$$

whereas a velocity fluctuation u similarly applied would produce a signal

$$e_v = [(K_u.i.R)_w - f_v(K_u.i.R)_h]\frac{u}{U}. \tag{3.3}$$

The hot wire required more compensation for thermal lag than the warm wire. This extra compensation was provided by the resistance-capacitance branch of the circuit labelled compensate.

Since the bridge was direct-coupled to the grids of the pre-amplifier stage, it was necessary to maintain the mean voltage level of the velocity and temperature signals near to earth potential. This was accomplished by backing off any residual voltage with the dry-cell-operated potentiometers in each output line.

In order to measure u and θ in a heated turbulent boundary layer, then, it was necessary to compute in advance the values of $(K_u.i.R)$ and $(K_\theta.i.R)$ at each station, so that the correct settings of the velocity and temperature potentiometers could be established. These computations were carried out for heating currents sufficient to maintain the mean temperatures of the wires at constant intervals above the mean temperature of the ambient air, using the data obtained during the measurements of the mean velocity and temperature profiles. In practice, only the velocity potentiometer setting had to be changed very much as the wire assembly was traversed through the boundary layer.

The use of these techniques made it necessary to construct wire assemblies having two identical parallel wires not more than 0·5 mm apart where the usual anemometer had only one wire. A typical double X-wire is depicted in figure 2. The very low velocities involved made it possible to employ hairpin loops of Wollaston wire (platinum core, 0·0025 mm in diameter), mounted by means of a jig so that they lay in parallel planes before etching, with no residual stress in the wires acting in planes at an angle to the hairpin. These loops were then brought within 0·5 mm of one another, and the outer casings of silver were removed by

etching them simultaneously. With a little luck, one could obtain parallel portions of the cores, held in tension and in correct alignment by the unetched portions of the hairpin loops of Wollaston wire. The supports were designed to make possible the adjustment of the wires in as many directions as possible and to

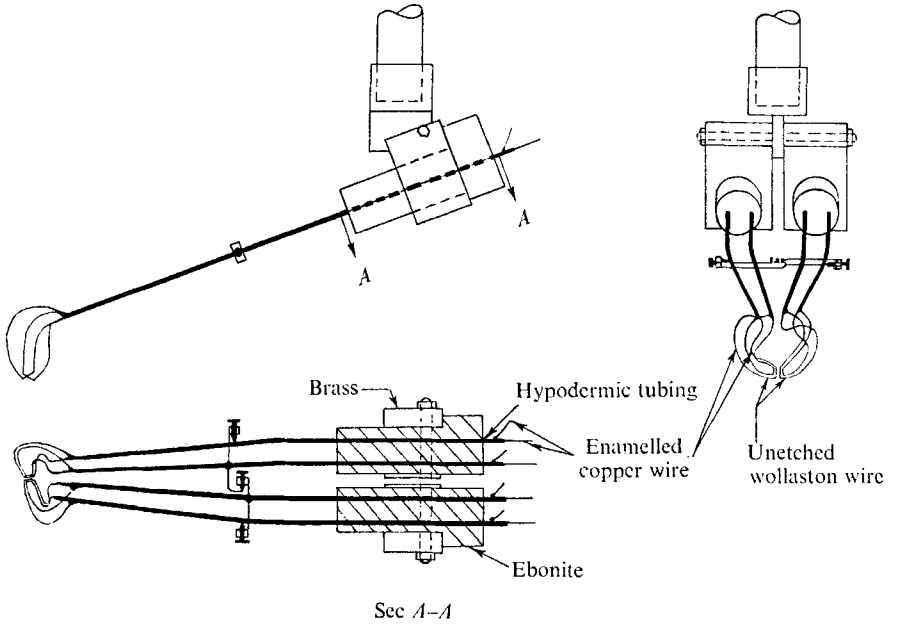

FIGURE 2. *X*-wire assembly and mounting.

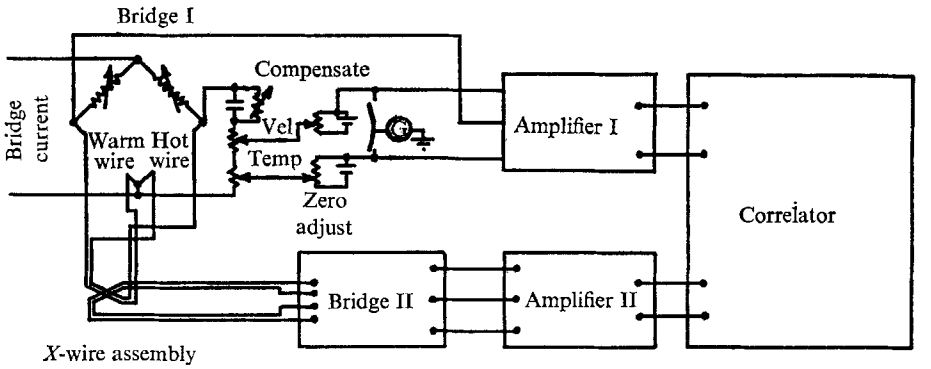

FIGURE 3. Block diagram of electronic circuits.

interfere with the flow as little as possible. Since the sensitive (etched) portion of the wire assembly was supported by lengths of Wollaston wire 10 mm long and a few hundredths of a mm in diameter, there was in fact very little interference with the flow over the heated wires. The etched portions were between 1·5 and 2 mm long.

The electronic circuits were based upon those developed by Townsend (1947) and Stewart (1951). Considerable modification of the switching and balancing

arrangements was made necessary by the comparatively complicated double-wire bridge circuits; and the low frequency response was improved to yield a flat response down to 1 hertz. Visual observations of the turbulent fluctuations suggested that a low frequency response flat down to 0·2 hertz would have been useful.

As finally developed, the circuitry made it possible to measure

$$\sqrt{\overline{u^2}}/U, \quad \sqrt{\overline{\theta^2}}/T, \quad \sqrt{\overline{w^2}}/\sqrt{\overline{u^2}}, \quad \overline{u\theta}/\sqrt{\overline{u^2}}\sqrt{\overline{\theta^2}}, \quad \overline{w\theta}/\sqrt{\overline{w^2}}\sqrt{\overline{\theta^2}},$$
$$\overline{uw}/\sqrt{\overline{u^2}}\sqrt{\overline{w^2}}, \quad \overline{w^3}/(\overline{w^2})^{\frac{3}{2}} \quad \text{and} \quad \overline{w\theta^2}/\sqrt{(\overline{w^2})}\,\overline{\theta^2}.$$

4. Experimental results

The unheated boundary layer

Mean velocity profiles obtained in the unheated boundary layer on the floor and on the roof of the wind tunnel are compared in figure 4 with the 'equilibrium' profile obtained by Klebanoff (1954) and with the 'universal' profile suggested by Clauser (1954). Distributions of $\sqrt{\overline{u^2}}$, $\sqrt{\overline{w^2}}$, $\overline{uw}/\sqrt{\overline{u^2}}\sqrt{\overline{w^2}}$ and $\overline{w^3}/(\overline{w^2})^{\frac{3}{2}}$ measured in the unheated layers did not reveal significant deviations from the shapes observed by Townsend and Klebanoff. This similarity is important only in that it demonstrates that the mechanisms of production, diffusion and dissipation of turbulent energy were present in a form not essentially different from that encountered at much higher Reynolds numbers.

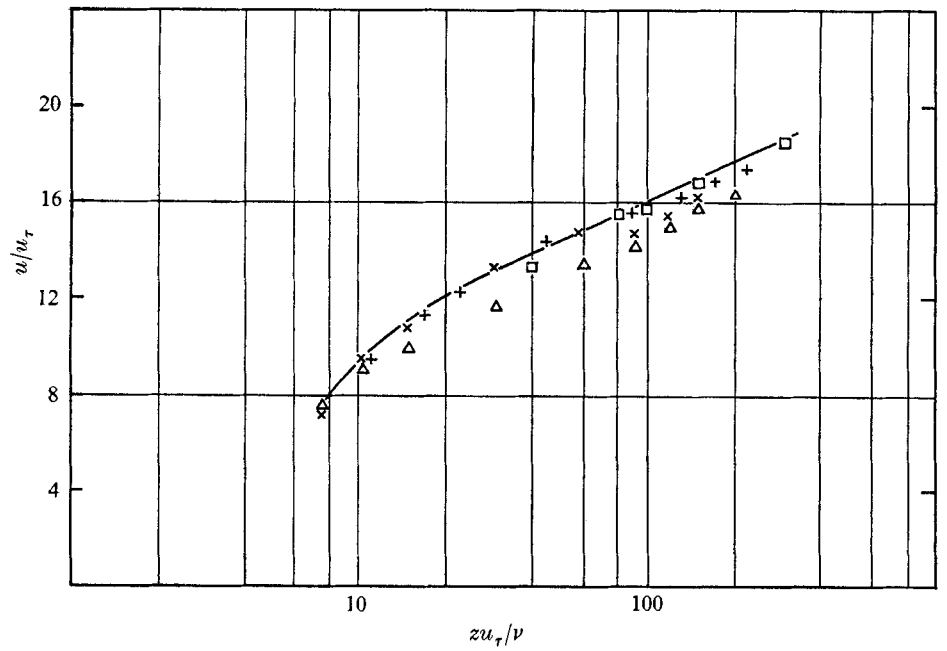

FIGURE 4. Mean velocity profiles in unheated tunnel. ——, Clauser; □, Klebanoff; △, roof, $U_0 = 150$ cm/sec, $x_h = 74$ cm; ×, roof, $U_0 = 150$ cm/sec, $x_h = 24$ cm; +, floor, $U_0 = 240$ cm/sec, $x_h = 74$ cm.

The boundary layer on the heated floor

The boundary layer on the floor of the tunnel was studied for two surface temperature discontinuities, 20 °C and 80 °C respectively above the temperature of the air entering the tunnel.

The direct effect of a 20 °C temperature rise upon the mean velocity distribution (figure 5) is seen to be limited to a slight deceleration of the layer very close to the floor. In conjunction with the reduced density in this region, this deceleration produces an increase in the displacement thickness of the boundary layer and a slight increase in the velocity in the outer part of the layer, outside the region where the temperature of the air has been changed.

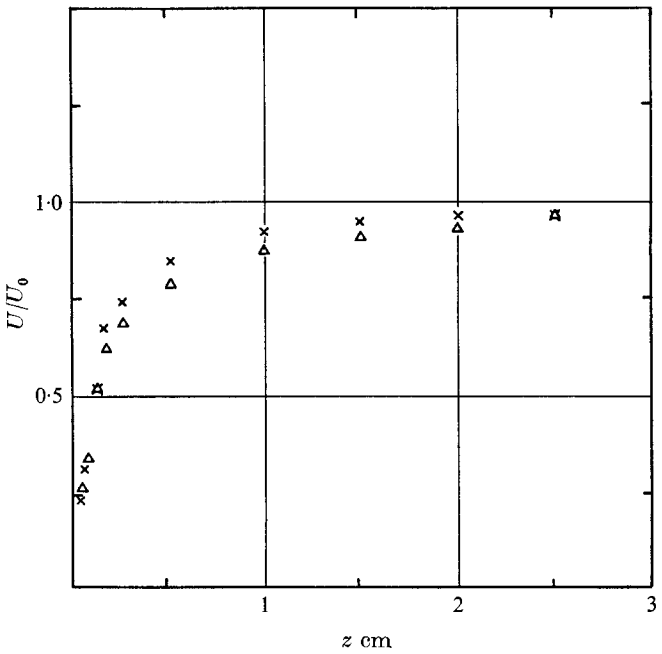

FIGURE 5. Mean velocity profile on heated floor. $U_0 = 240$ cm/sec.
△, $T_1 - T_0 = 0$ °C; ×, $T_1 - T_0 = 20$ °C.

Figure 6 shows that, sufficiently far downstream, the effect of the 80 °C discontinuity in the wall temperature is of the same character. It is interesting to compare the temperature distribution at $x_h = 74$ cm with that observed by Johnson (1957) in a similar configuration, where the temperature rise had the maximum value which did not produce detectable change in the distributions of mean velocity and longitudinal component of the turbulence. Priestley (1954) has shown that, for free convection in a perfect gas under circumstances such that the heat flux is constant with height and independent of molecular transport coefficients, so that the motion on the turbulent scale is determined by the heat flux, dimensional analysis requires that $\log(T/T_0) \propto z^{-\frac{1}{3}}$. Using Johnson's

measurements and the temperature profiles obtained on the floor and on the roof of the tunnel 74 cm downstream of a strong surface temperature discontinuity,

$$\Phi = [\log(T/T_0)/\log(T_1/T_0)]\,(z/\delta_c)^{\frac{1}{3}}$$

is plotted against z/δ_c in figure 7, where T_1 is the surface temperature and δ_c is a thermal or convection thickness defined by

$$\delta_c = \int (U/U_0)\,(T-T_0)/(T_1-T_0)\,dz.$$

Johnson's profile serves as a reference, since the heat flux was chosen to have no effect upon the mean flow. Considering the factor of 50 in R between the two configurations, the shape of the profile on the floor downstream of the 80 °C dis-

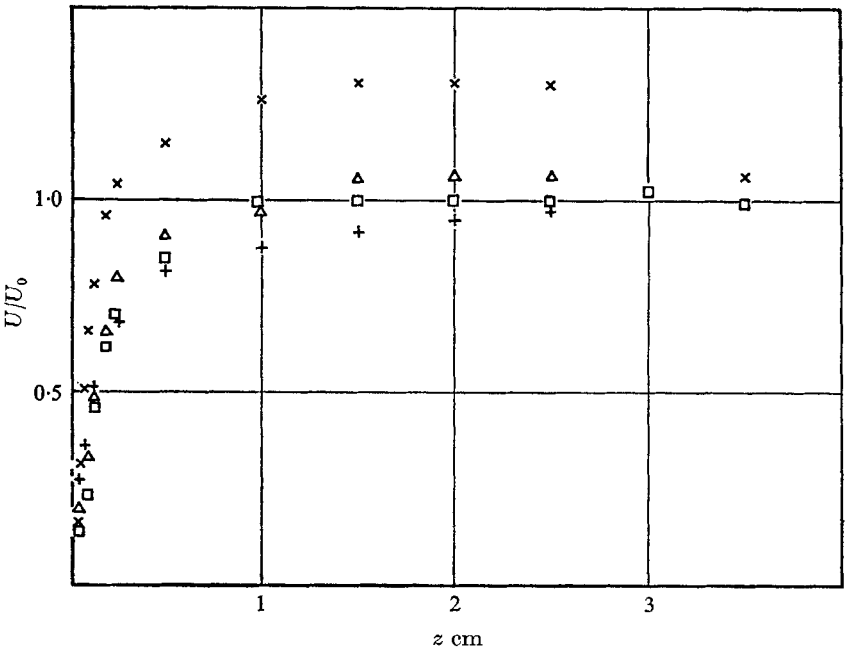

FIGURE 6. Mean velocity profiles on heated floor. U_0 = 240 cm/sec. T_1-T_0 = 0 °C: +, x_h = 74 cm. T_1-T_0 = 80 °C: □, x_h = 74 cm; △, x_h = 24 cm; ×, x_h = 14 cm.

continuity is not greatly affected. However, buoyant forces are seen to be dominant in the region $3 < z/\delta_c < 6$, producing a nearly constant value of Φ; and further evidence in support of this was provided by the character of the turbulent velocity fluctuations in this region, which were dominated by strongly skewed low frequency 'billows'. Φ could not be expected to be strictly constant in a layer of such small vertical extent; and in fact, Thomas & Townsend (1957) have noted that the hypotheses on which the $z^{-\frac{1}{3}}$ law rests are not entirely satisfied even when the free stream velocity goes to zero, that is, when $R \to -\infty$.

The only other significant dynamic effect of the heating at x_h = 74 cm on the floor is the sharp increase in $\overline{w^2}/\overline{u^2}$ at $z < 0{\cdot}5\,\delta_c$. This suggests a convective layer very close to the floor, controlled by local expansion processes and evidently

capable of distorting the mean temperature profile. It is interesting to note that Johnson observed a similar phenomenon (which he attributed to experimental error) even when the value of R was so low that no other dynamical effect was produced.

Thus the flow far downstream of the 80 °C floor temperature discontinuity is not very sensitive to the intensity of the heat flux passing through it. However,

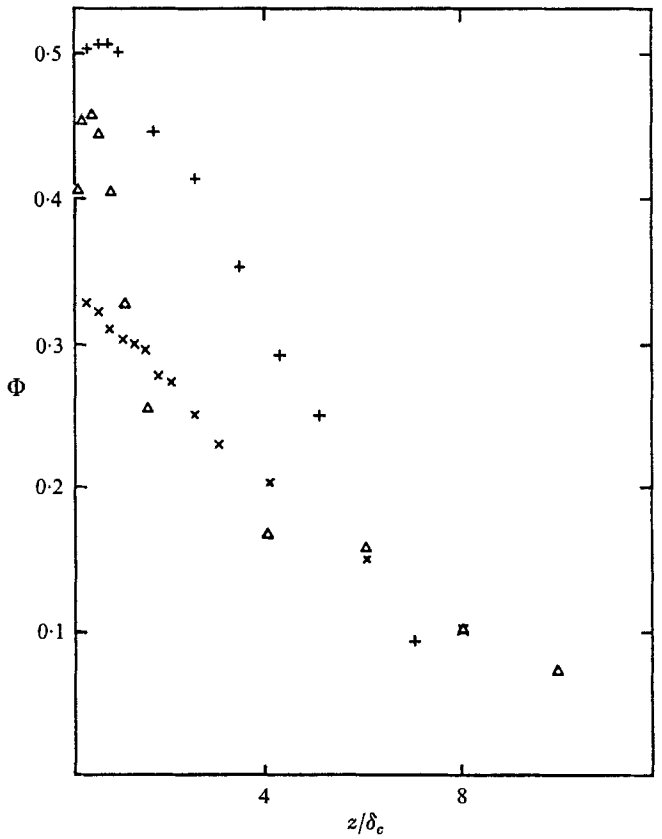

FIGURE 7. △, floor, Nicholl; +, roof, Nicholl; ×, Johnson.

figure 6 makes it clear that, immediately downstream of the surface temperature discontinuity, a transition flow of entirely different character has been generated. In particular, the velocity in the boundary layer region reaches a maximum of $1{\cdot}3U_0$ at a point far outside the layer in which the mean temperature has been changed. Rankine (1950) has observed a similar 'wall jet' downstream of an intense line source of heat lying in the floor surface and normal to the free stream velocity. In order to ascertain the cause of this anomaly, we must examine the effect which the strong heating has had on the turbulent structure of the flow.

The topography of the first 25 cm downstream of the surface temperature discontinuity is described in figure 8. The outer edge of the heated layer grows through the momentum boundary layer, reaching approximately 35 % of the

thickness of the momentum layer at $x_h = 14$ cm. The shape of the streamlines has been obtained from the mass balance equation (2.3), using the measured distributions of U, $\sqrt{u^2}$, $\sqrt{w^2}$, $\overline{u\theta}$ and $\overline{w\theta}$ (figures 6, 9, 10, 12 and 13). Again, attention is drawn to the strongly perturbed mean velocity field in the region outside the temperature boundary layer, where the mean flow divergence is everywhere zero. Only within 0·5 cm of the floor is the density flux significant. At $x_h = 14$ cm, the $\overline{w\theta}$ correlation changes sign very close to the floor, which

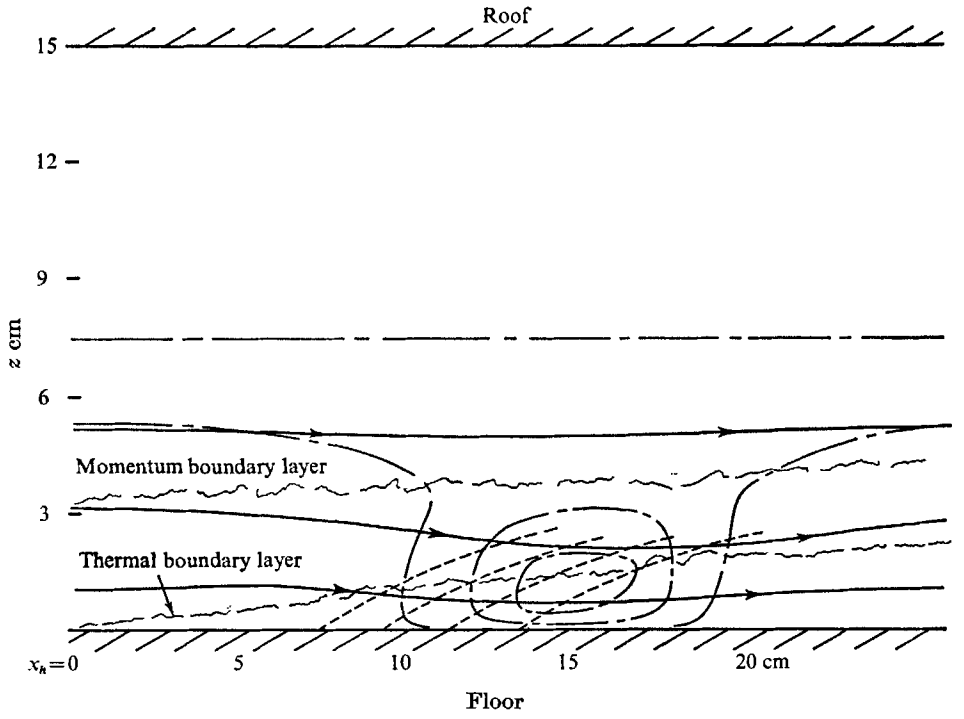

FIGURE 8. ⟶, streamline; - - - - -, convection column; — · —, pressure contour.

suggests that the vertical component of turbulent motion in this region must be associated with work of expansion. However, even here the contribution of the turbulent mass flux represented by $\partial\overline{w\theta}/\partial z$ is an order of magnitude smaller than the contributions to the mass balance associated with the observed gradients of mean velocity and mean density in the field.

In order to explain the sudden appearance of this relatively intense wall jet, we have to examine the horizontal and vertical momentum balances (equations (2.4), (2.5)) in the vicinity of $x_h = 14$ cm, inserting data obtained from the measured distributions of U, $\sqrt{u^2}$, $\sqrt{w^2}$, $\overline{u\theta}$, $\overline{w\theta}$ and $\overline{uw}$ (figure 12). Throughout the region immediately upstream of the plane $x_h = 14$ cm, the convection terms of the x momentum equation are dominated by $\partial(\rho U^2)/\partial x$. A balance requires the pressure to decrease in the direction of the flow, so that a pressure minimum is found at about $z = 1{\cdot}5$ cm. In the plane $x_h = 14$ cm, the pressure decreases from

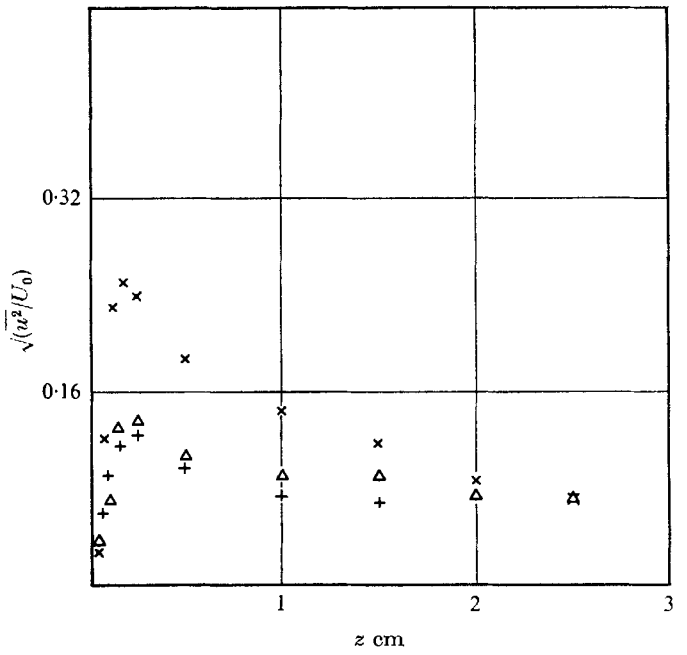

FIGURE 9. Distribution of longitudinal component of turbulent velocity on heated floor. $U_0 = 240$ cm/sec. $T_1 - T_0 = 0\,°C$: +, $x_h = 74$ cm. $T_1 - T_0 = 80\,°C$: △, $x_h = 74$ cm; ×, $x_h = 14$ cm.

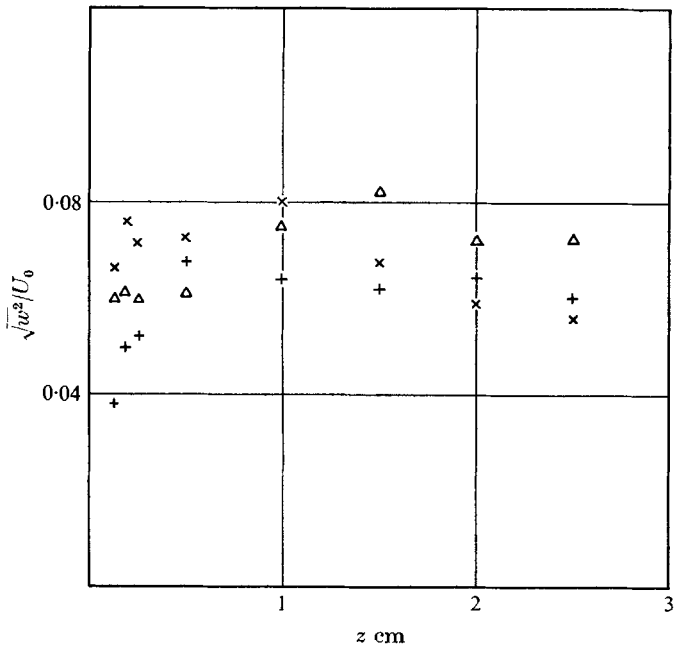

FIGURE 10. Distribution of vertical component of turbulent velocity on heated floor. $U_0 = 240$ cm/sec. $T_1 - T_0 = 0\,°C$: +, $x_h = 74$ cm. $T_1 - T_0 = 80\,°C$: △, $x_h = 74$ cm; ×, $x_h = 14$ cm.

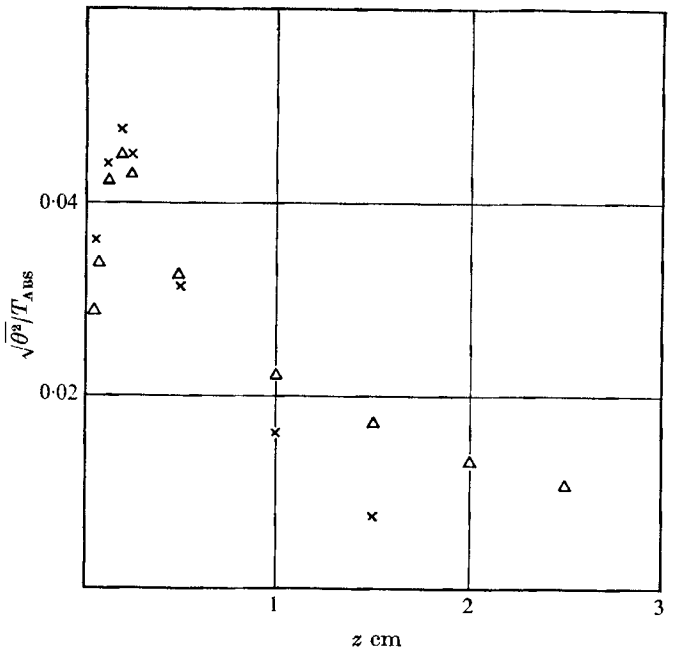

FIGURE 11. Distributions of temperature fluctuations on heated floor. $U_0 = 240$ cm/sec. $T_1 - T_0 = 80\,°C$: △, $x_h = 74$ cm; ×, $x_h = 14$ cm.

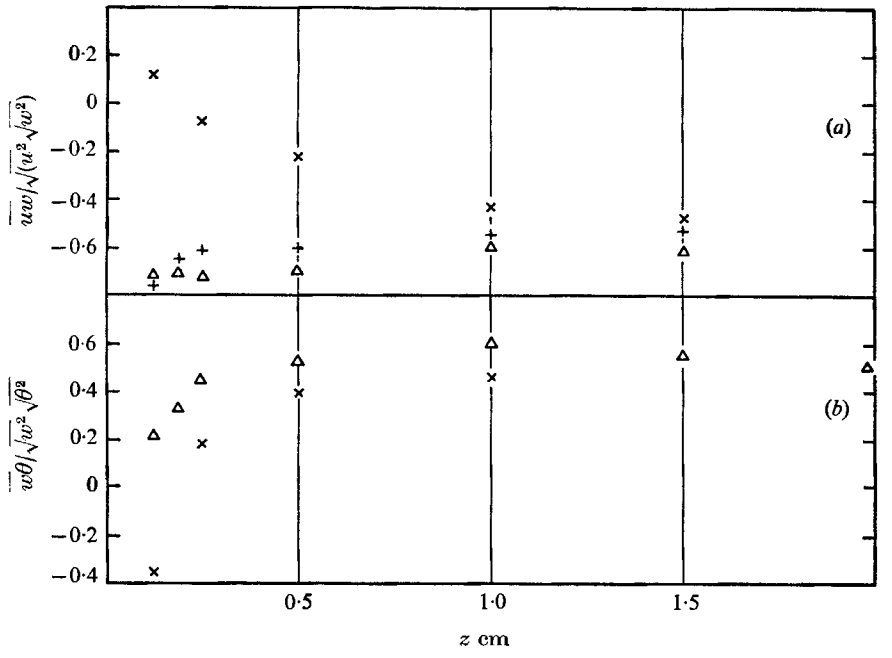

FIGURE 12. Structural correlations on heated floor. $U_0 = 240$ cm/sec. (*a*) $T_1 - T_0 = 0\,°C$: +, $x_h = 74$ cm. (*a*) and (*b*) $T_1 - T_0 = 80\,°C$: △, $x_h = 74$ cm; ×, $x_h = 14$ cm.

a value about 5 cm of air less than the value for hydrostatic equilibrium at the floor to a minimum of 20 cm of air below the hydrostatic value at $z = 1{\cdot}5$ cm. The pressure then increases with z to reach hydrostatic value in the vicinity of $z = 5$ cm. The origin of this anomalous vertical pressure distribution must lie in the flow structure on the turbulent scale of motion.

If the turbulent structure at $x_h = 14$ cm is compared with the structure far downstream, it will be seen that the u component is 80 % higher at $x_h = 14$ cm over the whole of the low-pressure region, while $\sqrt{w^2}$ is increased by 25 % over the region $z < 0{\cdot}5$ cm; but the increase of $\sqrt{w^2}$ relative to the value in the unheated boundary layer is as much as 100 %. The correlation coefficient $\overline{u\theta}/\sqrt{u^2}\sqrt{\theta^2}$ is relatively high close to the floor (figure 13), while the coefficient $\overline{w\theta}/\sqrt{w^2}\sqrt{\theta^2}$ is reduced in the low pressure region and changes sign very close to the floor. The coefficient $\overline{uw}/\sqrt{u^2}\sqrt{w^2}$ approaches zero close to the floor, and its value is very much reduced over the whole low pressure region.

On the basis of these measurements, intense local convective activity is proposed as the origin of the low pressure region. When the boundary layer first encounters a heated surface, the very strong conductive influx of heat will create a layer of hot air in which the mean horizontal velocity and the turbulent intensity level are slightly reduced due to increased kinematic viscosity. The upper edge of this layer is bombarded by the boundary layer turbulence, and any perturbation of this edge is bound to grow rapidly under the influence of the highly unstable density gradient. The rising hot air would tend to concentrate into columns, allowing the cold air to penetrate between them and down towards the surface. The variation of $\overline{w\theta}/\sqrt{w^2}\sqrt{\theta^2}$ close to the floor shows that the convective activity is sufficiently intense that adiabatic expansion at the roots of the columns is affecting the local temperature, and therefore the local pressure. The vertical pressure gradient, then, is controlled by the dynamics of these convecting columns, and cold air is accelerated into the low pressure regions between the columns. This relatively organized and regular structure is the result of the collapse of the interface between the hot bubble of air at the leading edge and the cold air of the boundary layer; and the structure does not survive further downstream where the increased velocity shear associated with the wall jet would increase the ordinary turbulence level and restore a more normal turbulent structure.

The proposed structure on the turbulent scale of motion requires the generation of comparatively strong upward currents close to the floor; but these are confined to the convective columns and do not imply a strong mean divergence of the flow. The vanishing of $\overline{uw}$ close to the floor shows that u and w are not closely coupled in this comparatively regular type of motion on a turbulent scale. Thus $\overline{u\theta}/\sqrt{u^2}\sqrt{\theta^2}$, which is chiefly associated with the inrushing jet, remains strongly negative close to the floor, while $\overline{w\theta}/\sqrt{w^2}\sqrt{\theta^2}$, depending on the convective columns, varies with z over a wide range.

The paths of the convecting columns and contours of constant pressure are sketched on figure 8. The upper limit of the low pressure region is controlled by

the mixing of the convecting columns with their surroundings. The $\overline{p'\partial u_i/\partial x_i}$ term in the heat balance equation, which represents the conversion of heat energy into mechanical energy on a turbulent scale of motion, is considerably larger than the net gain of heat by conduction in the region of $x_h = 12$ cm near the floor.

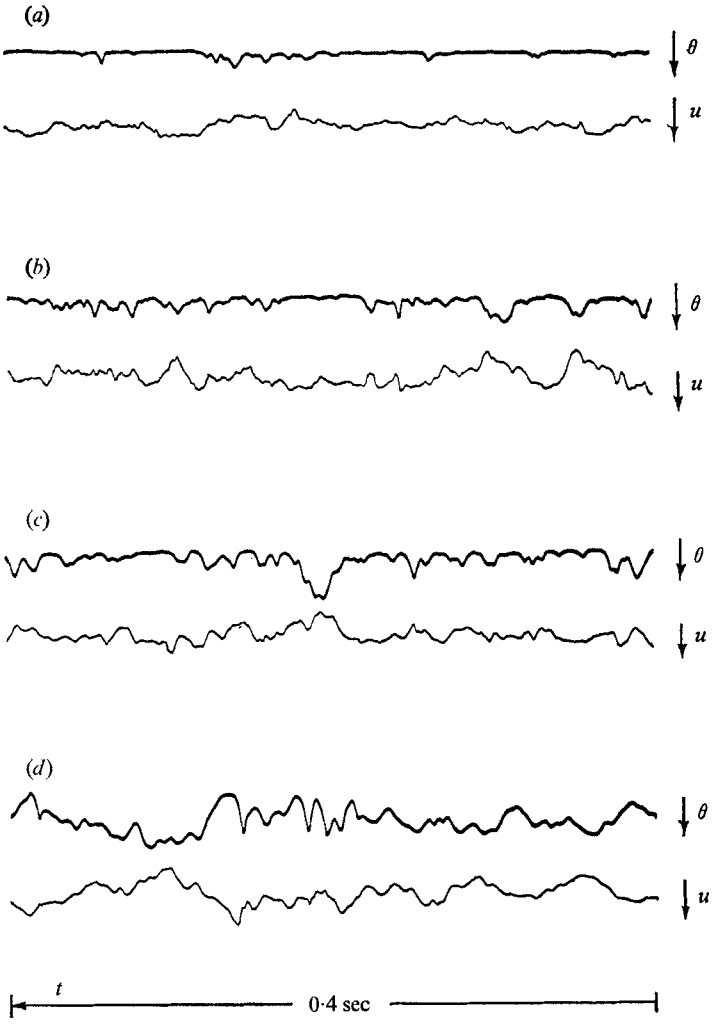

FIGURE 13. Oscillograms, floor. $U_0 = 240$ cm/sec, $x_h = 14$ cm, $T_1 - T_0 = 80\,^{\circ}$C. (*a*) $z = 1$ cm, $\overline{u\theta}/\sqrt{\overline{u^2}}\sqrt{\overline{\theta^2}} = -0{\cdot}27$. (*b*) $z = 0{\cdot}5$ cm, $\overline{u\theta}/\sqrt{\overline{u^2}}\sqrt{\overline{\theta^2}} = -0{\cdot}43$. (*c*) $z = 0{\cdot}25$ cm, $\overline{u\theta}/\sqrt{\overline{u^2}}\sqrt{\overline{\theta^2}} = -0{\cdot}68$. (*d*) $z = 0{\cdot}075$ cm, $\overline{u\theta}/\sqrt{\overline{u^2}}\sqrt{\overline{\theta^2}} = -0{\cdot}62$.

Downstream, the 'jet' is quickly decelerated by the adverse pressure gradient and by shear forces above and below. Whether the flow near the floor builds up to another collapse depends upon whether the flux of heat by conduction from the surface is sufficiently strong, at the prevailing turbulence levels, to establish convection columns.

Thus the effect of the work of expansion is to introduce a coupling between the free and forced convection modes which leads to the possibility of a series of short 'wall jets' downstream of the surface temperature discontinuity. Zeytou-

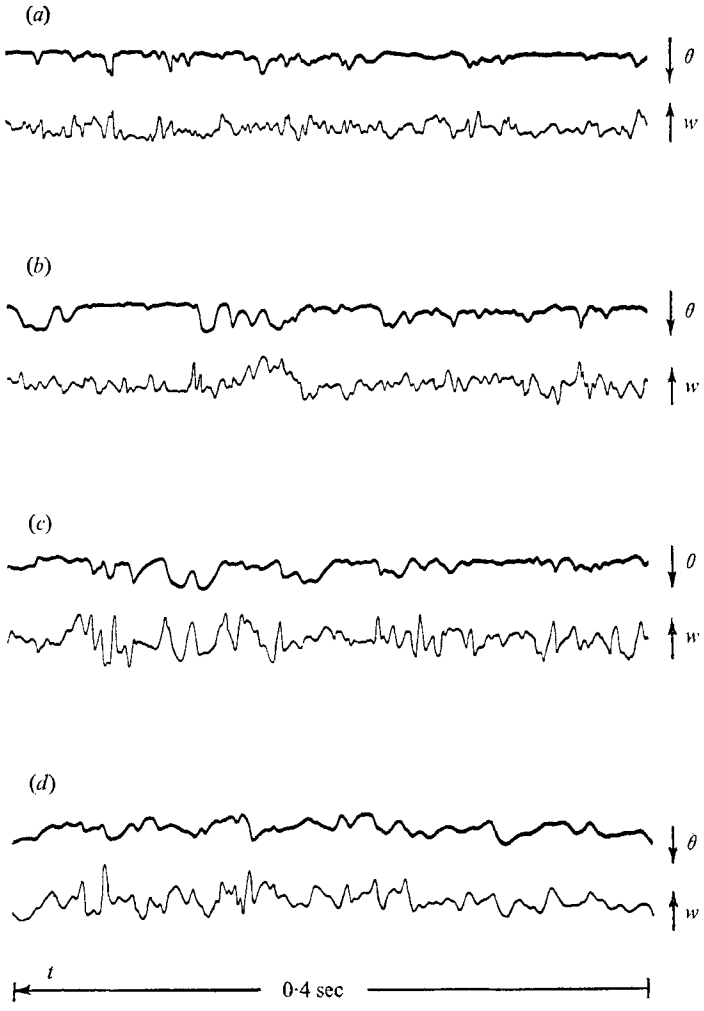

FIGURE 14. Oscillograms, floor. $U_0 = 240$ cm/sec, $x_h = 14$ cm, $T_1 - T_0 = 80\,°\text{C}$. (a) $z = 1$ cm, $\overline{w\theta}/\sqrt{w^2}\sqrt{\theta^2} = 0{\cdot}47$. (b) $z = 0{\cdot}5$ cm, $\overline{w\theta}/\sqrt{w^2}\sqrt{\theta^2} = 0{\cdot}39$. (c) $z = 0{\cdot}25$ cm, $\overline{w\theta}/\sqrt{w^2}\sqrt{\theta^2} = 0{\cdot}17$. (d) $z = 0{\cdot}125$ cm, $\overline{w\theta}/\sqrt{w^2}\sqrt{\theta^2} = -0{\cdot}36$.

nian (1968) has recently obtained a theoretical solution of the laminar boundary layer flow over a heated rectangle in a flat plate which displays a series of rising and descending vertical currents downstream as a result of similar coupling.

The boundary layer on the heated roof

The boundary layer along the roof of the tunnel was studied for a rise of 100 °C at a free stream velocity of 150 cm/s, and a rise of 94 °C at a free stream velocity of 190 cm/s. Figures 15–20 present some of the measured distributions of

U, T, $\sqrt{\overline{u^2}}$, $\sqrt{\overline{\theta^2}}$, $\sqrt{\overline{w^2}}$, $\overline{w\theta}$ and $\overline{uw}$, of which the first four have already appeared in Townsend (1957).

At the higher velocity, the effect of the temperature discontinuity on the velocity profile is similar to that obtained from a 20 °C discontinuity on the floor, though greater in magnitude because of the much stronger heating. The layers close to the roof are retarded, due to the increase in kinematic viscosity. This corresponds to an increase in displacement thickness of the boundary layer, the streamlines close to the roof are turned downward and the lower part of the layer is

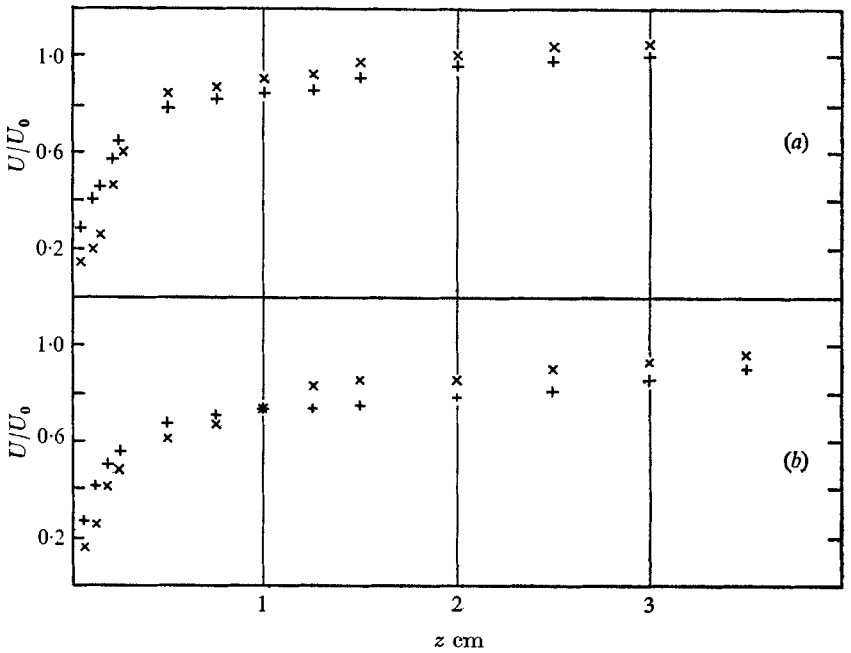

FIGURE 15. Mean velocity profiles on heated roof. U_0 = 190 cm/sec. +, $T_1 - T_0$ = 0 °C; ×, $T_1 - T_0$ = 94 °C. (*a*) x_h = 24 cm. (*b*) x_h = 74 cm.

accelerated. The temperature profile far downstream, plotted non-dimensionally on figure 7, reveals a heat trap very close to the roof and a relatively steep and uniform gradient in the outer regions. The heat trap is probably associated with the suppression of the turbulence which is observed in the layer $|z| < 0{\cdot}2$ cm, where the kinematic viscosity is 60 % higher than in the free stream. Further out, the larger scale eddies convecting heat away from the roof are required to do work against gravity and are weakened in consequence, so that the convective heat flux is reduced and the outward development of the thermal layer is retarded.

At 150 cm/s, the dynamical effects of the heat flux are again sufficient to produce a strong perturbation of the mean velocity profile. At first, the layer of air within 0·2 cm of the roof is retarded and the displacement thickness of the boundary layer is increased, as for the higher velocity. However, within a very short distance downstream, the intensity of the u and w components of the turbulent velocity is very sharply reduced, and the layer immediately adjacent

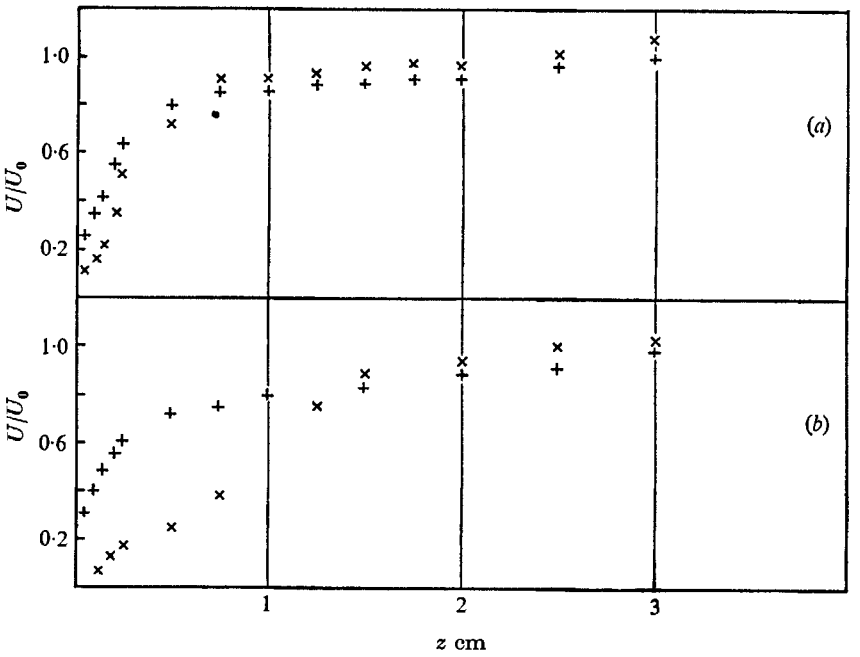

FIGURE 16. Mean velocity profiles on heated roof. U_0 = 150 cm/sec. +, T_1-T_0 = 0°C; ×, T_1-T_0 = 100°C. (*a*) x_h = 24 cm. (*b*) x_h = 74 cm.

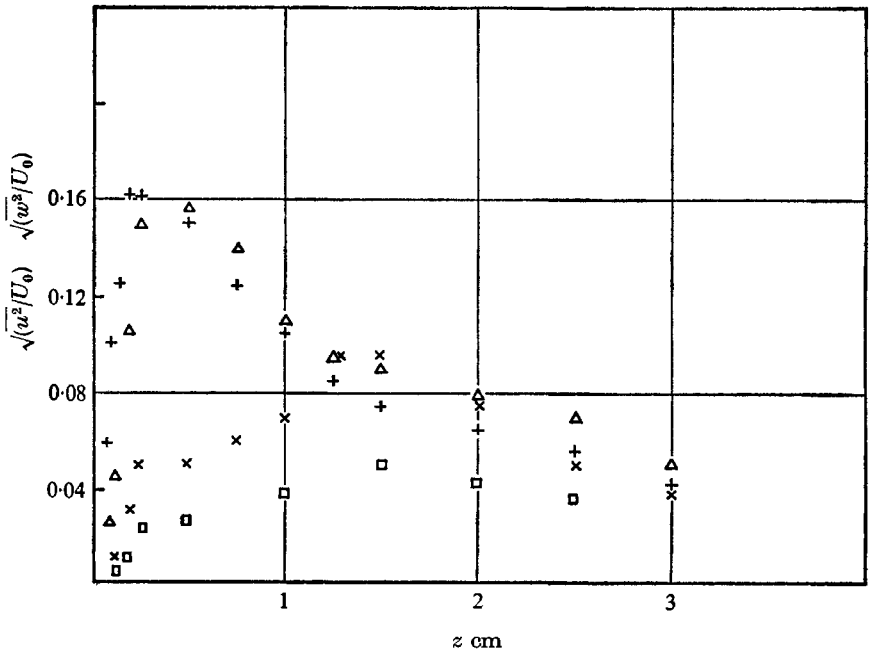

FIGURE 17. Distribution of turbulent velocity components on heated roof. U_0 = 150 cm/sec.

	x_h (cm)	T_1-T_0 (°C)	
+	24	0	$\sqrt{u^2}/U_0$
△	24	100	$\sqrt{u^2}/U_0$
×	74	100	$\sqrt{u^2}/U_0$
□	74	100	$\sqrt{w^2}/U_0$

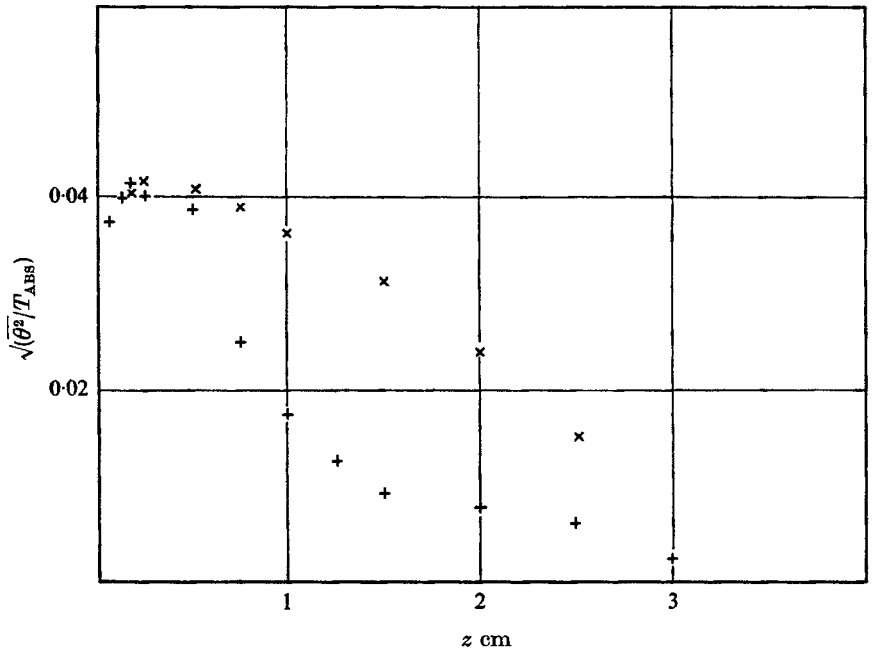

FIGURE 18. Distribution of turbulent fluctuations on heated roof. $U_0 = 150$ cm/sec, $T_1 - T_0 = 100\,°C$. +, $x_h = 24$ cm; ×, $x_h = 74$ cm.

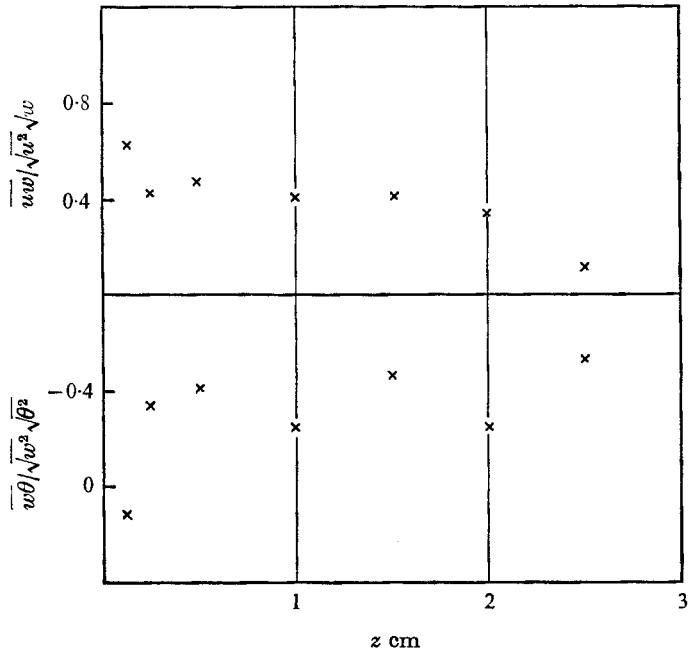

FIGURE 19. Structural correlations on heated roof. $U_0 = 150$ cm/sec, $x_h = 74$ cm, $T_1 - T_0 = 100\,°C$.

to the roof is thus 'disconnected' from the free stream. The subsequent rapid deceleration of this layer produces a strong vertical component of mean velocity which is responsible for the high values of $\sqrt{\theta^2}$ observed in the outer part of the boundary layer, in spite of the reduced intensity of the turbulence within 1·5 cm of the roof. The distribution of the structural correlations (figure 19) shows that,

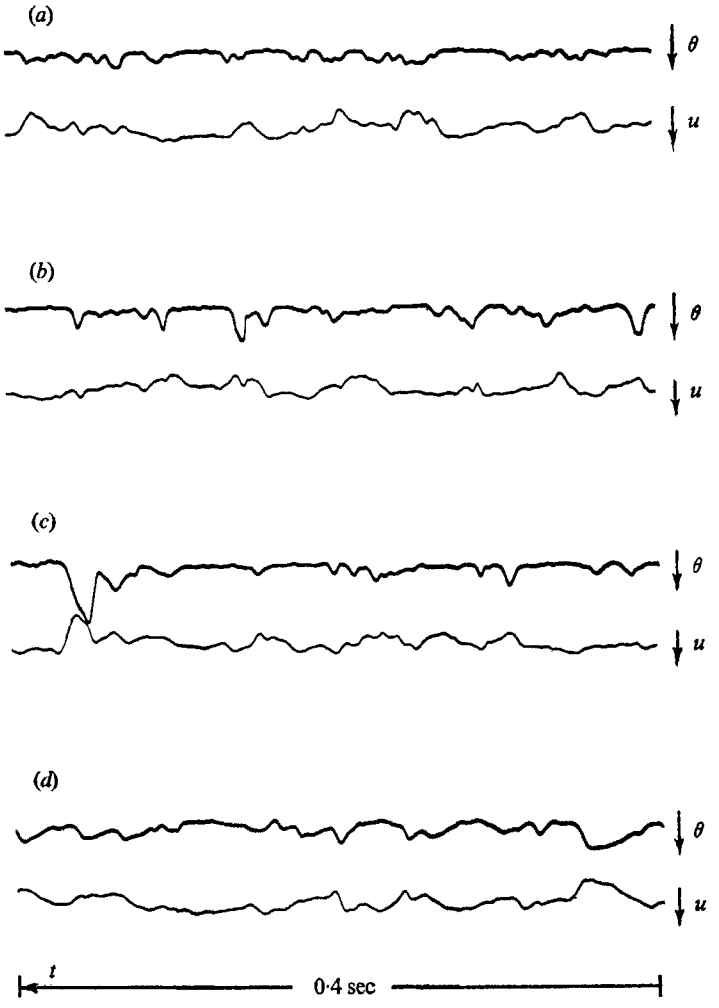

FIGURE 20. Oscillograms, roof. $U_0 = 150$ cm/sec, $x_h = 24$ cm, $T_1 - T_0 = 100$°C. (*a*) $z = 2{\cdot}5$ cm; (*b*) $x = 1{\cdot}5$ cm; (*c*) $z = 1{\cdot}0$ cm; (*d*) $z = 0{\cdot}5$ cm.

except in the region of expansion immediately below the roof, the turbulent structure had *not* been changed significantly in character by the heat flux.

Though the numerical value of any Richardson number relevant to the region where the turbulence collapses is very much less than one, the energy supply to the turbulent eddies is evidently no longer sufficient to cope with the extra work against the gravitational field required of the turbulent motion in the

stable density gradient. It might be thought that, because the turbulent mechanical energy per unit volume is a very small fraction of the rate of production and the rate of dissipation of turbulent mechanical energy per unit volume per second near the boundary, and less than the rates of supply and withdrawal in the outer layer, the turbulence level would therefore be very sensitive to slight changes in the boundary conditions. However, this does not seem to be the case in general. The Reynolds stress, which controls the rate of production of turbulent energy, has seemed to have a relatively large time constant, so that the local stress is a function of conditions in the flow and on the boundary for some distance upstream.

From an analysis of these and other experiments, Townsend (1957) has suggested that the 'critical' value of the appropriate Richardson number is of the order of 0·1. This low value implies that the eddies which control the Reynolds stress must have a relatively low energy level and a form such that they have to work relatively hard against the gravitational field—that is, they must be of large vertical extent. This is in agreement with the hypotheses of modern theories of turbulent shear flow (Townsend 1956).

5. Conclusions

The experiments reported in this paper have demonstrated that the expansion of a fluid due to temperature changes associated with the convection of heat from a solid surface by a turbulent boundary layer may have important dynamical consequences.

In the case of an unstable mean temperature distribution, the vigorous expansion associated with a strong influx of heat by conduction from the surface may lead to a fine-scale motion of convection columns originating at the unstable interface between the hot and cold fluid streams and rising with sufficient velocity that the mean pressure in the vicinity is significantly reduced. In the case of a stable mean temperature distribution, the turbulence is required to transport a weight flux against the gravitational field, and the work required may be more than the source of turbulent energy can supply.

Though dynamical similarity could be expected to have only very local validity in such a thoroughly inhomogeneous field, it is interesting to compare the relative importance of these phenomena in boundary layer flows of air and water, with the aid of the relevant non-dimensional parameters.

The deformation of the temperature profile observed in the region $3 < z/\delta_c < 6$ at $x_h = 74$ cm for the 80 °C discontinuity on the floor is associated with free convection governed by the Grashof number $\beta.g.l^3(T_1-T_0)/\nu^2$. Although β, the thermal coefficient of expansion, is much smaller in water than in air, the effect of this is more than compensated for by the very small kinematic viscosity ν of water; so that for a given temperature discontinuity the Grashof number would be larger and the $z^{-\frac{1}{3}}$ law would be more nearly satisfied in water than in air.

The generation of convection columns at the unstable interface over the heated floor in the region $5 < x_h < 15$ cm is probably influenced by thermal conductivity K, so that the relevant parameter would be the Rayleigh number

$\beta.g.l^3(T_1-T_0)/\nu.K$; and the phenomena would be generated for a lower mean temperature difference in water than in air.

It should be remembered, of course, that due to the difference in the values of $\rho.C_p$ in water and air, the flux of heat required to maintain a given temperature difference across a boundary layer at a given free stream velocity would be enormously greater in water than in air.

The perturbation of the flow pattern by the influx of heat in the unstable case would be characterized by a sort of perturbation Euler number $\sqrt{\overline{p'^2}}/\rho U_0^2.\sqrt{\overline{p'^2}}$ is related to the kinetic energy per unit volume generated in the convection columns, which in this region is a function of the inhomogeneity $\beta(T_1-T_0)$, to the approximation involved in equations (2.1), (2.2). Though the pattern of the kinematics of the collapse of the unstable interface is due to the gravitational field, the intensity of the movement is controlled by the coefficient of thermal expansion of the fluid. On this basis, the perturbation would be much less in water than in air, for a given temperature difference across the boundary layer.

Finally, the significance of the work done by the turbulence against the gravitational field in the stably stratified case is measured by the Richardson number $\overline{\rho'w}.g/\rho.\overline{uw}(\partial U/\partial z)$, hence, in a given velocity and temperature field, by the thermal coefficient of expansion of the fluid, which is an order of magnitude greater in air than in water. It follows that it is unlikely that turbulence would be suppressed by density gradients of thermal origin in water.

The experimental results presented in this paper are drawn from a doctoral dissertation presented to the University of Cambridge in 1958. The author would like to express his gratitude to Dr A. A. Townsend for the stimulus of his example and for much good advice; and also to the National Research Council of Canada for financial support during his stay in Cambridge.

REFERENCES

Batchelor, G. K. 1953 *Quart. J. Roy. Met. Soc.* **79**, 223.
Clauser, F. H. 1954 *J. Aero. Sci.* **21**, 91.
Ellison, T. H. 1957 *J. Fluid Mech.* **2**, 456.
Johnson, D. S. 1957 *J. Appl. Mech.* **24**, 2.
Klebanoff, P. S. 1954 *N.A.C.A. Tech. Note* 3178.
Priestley, C. H. B. 1954 *Australian J. Phys.* **7**, 176.
Rankine, A. O. 1950 *Proc. Phys. Soc. Lond.* B**63**, 225.
Richardson, L. F. 1920 *Proc. Roy. Soc. Lond.* A**97**, 354.
Stewart, R. W. 1951 *Proc. Camb. Phil. Soc.* **47**, 146.
Thomas, D. & Townsend, A. A. 1957 *J. Fluid Mech.* **2**, 473.
Townsend, A. A. 1947 *Proc. Camb. Phil. Soc.* **43**, 560.
Townsend, A. A. 1951 *Proc. Roy. Soc. Lond.* A**209**, 418.
Townsend, A. A. 1956 *The Structure of Turbulent Shear Flow.* Cambridge University Press.
Townsend, A. A. 1957 *J. Fluid Mech.* **3**, 361.
Zeytounian, R. K. 1968 *La Recherche Aérospatiale*, **127**, 4.